Annual Review of Materials Research

Polymers Resist Fatigue Crack Growth by Deconcentrating Stress

Jason Steck, Christine Heera Ahn, and Zhigang Suo

John A. Paulson School of Engineering and Applied Science, Harvard University, Cambridge, Massachusetts, USA; email: suo@seas.harvard.edu

Annu. Rev. Mater. Res. 2025. 55:9.1–9.26

The *Annual Review of Materials Research* is online at matsci.annualreviews.org

https://doi.org/10.1146/annurev-matsci-101922-122133

Keywords

polymer, fracture, fatigue, stress deconcentration, fatigue threshold, soft materials

Abstract

When a material is cyclically loaded, an amplitude of load exists, called the threshold, below which a crack does not grow. In a polymeric material, physical interactions between polymer chains are much weaker than covalent bonds between repeat units along an individual chain. Consequently, when a crack impinges on a chain, high tension transmits along a long length of the chain. Breaking a single covalent bond dissipates the energy stored in that long length. The longer the length over which high tension transmits, the higher the threshold. Here we review how stress deconcentrates in diverse polymeric materials, including polymer networks, particle-reinforced elastomers, glassy polymers, semicrystalline polymers, phase-separated polymers, and composites. Ample opportunities exist for investigation and innovation.

1. INTRODUCTION

1.1. Characterizing Fatigue Crack Growth in a Material

In 1958, Alan Thomas, of the British Rubber Producers' Research Association, introduced a method to characterize fatigue crack growth in a material (1). The material is precut with a crack and cyclically loaded (**Figure 1*a***). The load is represented by the energy release rate, G (2). As the load cycles in time, so does the energy release rate (**Figure 1*b***). As the energy release rate cycles with a fixed amplitude, the crack length c increases with the number of cycles, N (**Figure 1*c***). After a period of transient growth, the crack attains a steady-state growth per cycle, dc/dN. This steady state is marked as a data point on the plane of dc/dN and G (**Figure 1*d***). When the experiment is repeated for many amplitudes of G, the data points are connected as a curve on the plane of dc/dN and G. Thomas demonstrated this method using elastomers. Paris and others (3) independently demonstrated the method using metals.

An amplitude of energy release rate exists, called the threshold, G_{th}, below which the crack does not grow in a steady state (4). When the amplitude of the energy release rate exceeds the threshold, $G > G_{th}$, the steady-state growth per cycle increases with G. The crack growth per cycle becomes too large to attain a steady state when G reaches a critical value, G_c, corresponding to the toughness measured under a monotonic load. This review is devoted to the threshold, G_{th}.

Accurately measuring the threshold is challenging. The steady-state crack growth rate is estimated as the total crack growth divided by the total number of cycles. The resolution of total crack growth is set by the resolution of the microscope. The total number of cycles is limited by the time

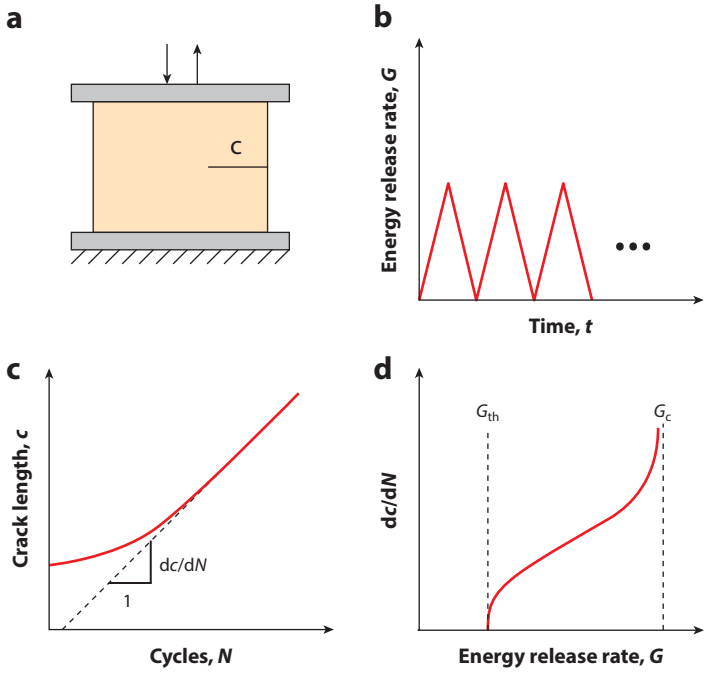

Figure 1

Crack growth in a material under cyclic load. (*a*) The material contains a precut crack (C) and is subject to cyclic load. (*b*) The load history is represented by the energy release rate G as a function of time. (*c*) Crack length as a function of the number of cycles. (*d*) The steady-state crack growth per cycle, dc/dN, as a function of G.

available to the experimentalist. For example, let the resolution of the crack length be 10 μm and the number of cycles be 10,000. The resolution of the crack growth rate is thus 10^{-9} m/cycle. If the resolution is too coarse, then the measurement will overestimate the threshold. In the literature, the resolution of the crack growth rate varies considerably, commonly ranging from 1 nm/cycle to 1 μm/cycle (5, 6). One should be careful in comparing thresholds reported in different papers.

1.2. Hysteresis Enhances Toughness but Not Threshold

Soon after the initial work of Thomas, experiments accumulated for various elastomers (7–10). These elastomers had thresholds of approximately 50 J/m^2, but their toughnesses were orders of magnitude higher (**Figure 2*a***).

The large difference between threshold and toughness is caused by inelastic deformation. Stretch a sample and then unload; the unloading curve is beneath the loading curve (**Figure 2*b***). This inelastic behavior is called hysteresis, where the area between the two curves is the energy dissipated. Inelasticity results from various processes, including frictional sliding between polymer chains, strain-induced crystallization, and detachment of polymer chains from reinforcing particles (6, 11–13).

On the basis of experimental data available at the time, Lake & Thomas (14) noted that hysteresis enhances toughness but not threshold (**Figure 2*c***). For example, friction between polymer chains is reduced when an elastomer imbibes a solvent of low viscosity. The toughness of the swollen elastomer is similar to the threshold of the dry elastomer (15–17). Additionally, strain-induced crystallization greatly amplifies toughness but not threshold (Section 5.2). As a more recent example, when an alginate/polyacrylamide hydrogel is stretched, ionic cross-links of the alginate network dissociate. This mechanism of inelasticity amplifies the toughness to 8,000 J/m^2, but the threshold is only 53 J/m^2 (18, 19). This threshold is close to the threshold of a pure polyacrylamide (PAAm) hydrogel, which is on the order of 10 J/m^2 (20, 21). When the

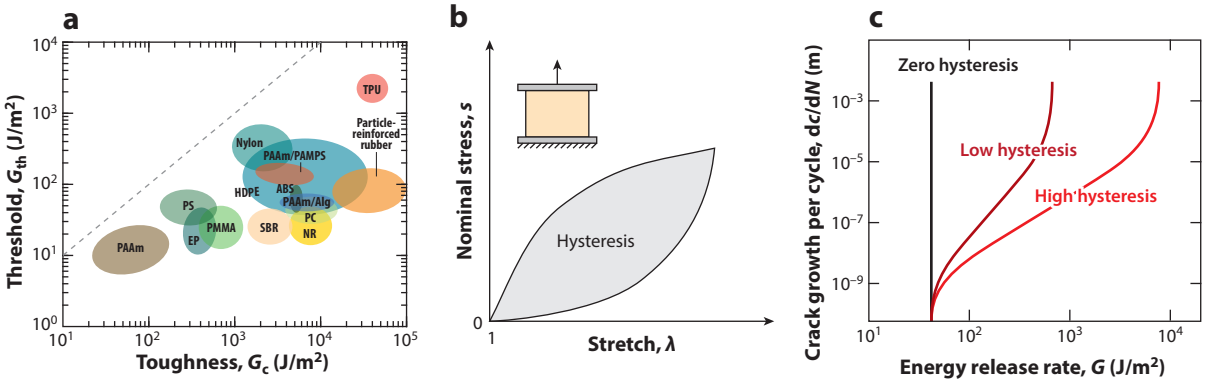

Figure 2

Threshold, toughness, and hysteresis. (*a*) Various polymeric materials are plotted on the plane of threshold G_{th} and toughness G_c (22, 23). A dashed line is drawn where the threshold equals the toughness. Data for nylon, polystyrene (PS), polycarbonate (PC), styrene-butadiene rubber (SBR), poly(methyl methacrylate) (PMMA), epoxy (EP), and acrylonitrile butadiene styrene (ABS) from Reference 22. Data for natural rubber (NR) from References 9 and 24. Data for high-density polyethylene (HDPE) from References 22, 25, and 26. Data for particle-reinforced rubber from References 4, 5, and 27–30. Data for polyacrylamide/poly(2-acrylamido-2-methylpropanesulfonic acid) (PAAm/PAMPS) from Reference 31. Data for thermoplastic polyurethane (TPU) from References 32–34. Data for polyacrylamide/alginate (PAAm/Alg) from (18, 19). Data for polyacrylamide (PAAm) from References 20, 21, and 35. (*b*) The loading and unloading curves of an inelastic material do not overlap. This behavior is called hysteresis. (*c*) For many polymeric materials, hysteresis amplifies toughness but not threshold.

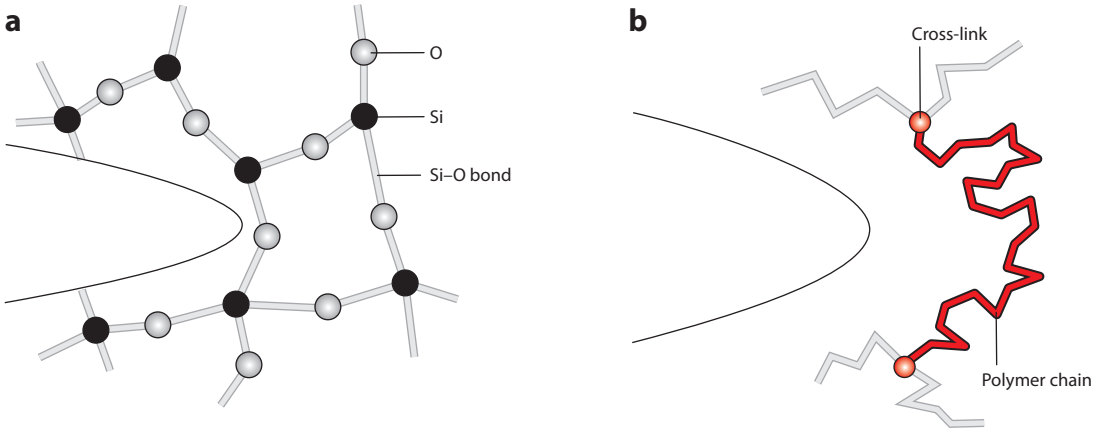

Figure 3

Molecular processes of crack growth. (*a*) A crack impinging on a Si–O bond in silica. (*b*) A crack impinging on a polymer chain in a polymer network.

amplitude of the energy release rate is between the threshold and toughness, hysteresis reduces the crack growth per cycle. The claim that hysteresis does not enhance threshold is often true, but below we discuss examples for which this is not true (Section 5).

1.3. Silica Concentrates Stress

Griffith (36) studied crack growth in silica under monotonic load. Silica is a network of Si–O bonds (**Figure 3*a***). Cut a crack in a sheet of silica and apply a load. The crack advances by breaking a single plane of Si–O bonds. That is, the crack tip concentrates stress to the scale of individual atoms. Atomic bonds off the plane of the crack remain elastic as the crack grows. The elasticity is visible: After fracture, the two halves of silica fit together. Consequently, the toughness of silica corresponds to the covalent energy per unit area in a layer of atomic bonds, which is on the order of $1\ \mathrm{J/m^2}$.

Later work showed that, under cyclic loading, cracks in glasses and ceramics can grow at energy release rates below the material's toughness (37). However, these materials have thresholds close to their toughnesses; the threshold is commonly half of the toughness. By contrast, rubbers and metals have thresholds 10 to 1,000 times lower than their toughnesses. Perhaps for this reason, fatigue crack growth in brittle materials has not been studied to the same extent as that in tough materials.

1.4. Polymer Networks Deconcentrate Stress

Lake & Thomas (14) introduced a model of the threshold of a polymer network. In a polymer network, cross-links divide each polymer into many segments, which we call chains. Consider a crack impinging on a polymer chain (**Figure 3*b***). Stretching the material causes high tension in the chain. Because the covalent bonds along the polymer chain are much stronger than the interactions between chains, high tension is transmitted along the entire length of the chain. Where the chain meets a cross-link, the high tension is distributed among two or more chains. That is, the cross-link concentrates stress from the network to the chain that bridges the crack. When the chain breaks at a single covalent bond, the energy stored in the entire chain is released. Consequently, the threshold scales with the covalent energy per unit area of a layer of polymer chains:

$$G_{\mathrm{th}} = \alpha n^{1/2} l J / v, \qquad 1.$$

where α is a prefactor of order unity, n is the number of repeat units per chain, l is the length of the repeat unit, J is the chemical energy of a covalent bond along the chain, and v is the volume per bond. The longer the polymer chain, the higher the threshold. In practice, energy can be released in more than a single layer of polymer chains, where the scalar coefficient α represents the number of layers of polymer chains that release energy during crack growth.

Weak interchain interaction enables high tension to transmit over the length of a polymer chain. That is, a polymer network deconcentrates stress. This behavior should be compared with how silica concentrates stress. Silica is a network of Si–O bonds (**Figure 3*a***). Consider a crack impinging on a Si–O bond. Stretching the material causes high tension in the Si–O bond. Every silicon atom is bonded to four oxygen atoms such that high tension is concentrated to a few bonds at the crack tip. Consequently, the threshold scales with the covalent energy per unit area to rupture a layer of Si–O bonds:

$$G_{\text{th}} = \alpha l J / v. \qquad 2.$$

In effect, a silica network is a polymer network of one repeat unit per chain.

Incidentally, polydimethylsiloxane (PDMS) is an elastomer of long chains of Si–O bonds. Each silicon atom is also bonded with two CH_3 groups, which mediate weak physical interactions between polymer chains. The weakness in the interactions between the chains deconcentrates stress along each chain such that PDMS has a much higher threshold than silica (15).

The modulus of a polymer network is given by

$$E = 3\mathrm{k}T/(nv), \qquad 3.$$

where k is Boltzmann's constant and T is temperature (38). Increasing the chain length increases the threshold but decreases the modulus. A combination of Equations 2 and 3 gives

$$E \propto {G_{\text{th}}}^{-1/2}. \qquad 4.$$

This relation quantifies the modulus–threshold conflict for polymer networks (39). Conflicts between material properties are common in all materials (40). For example, materials with higher strength also typically have lower toughness (41). In this review, we consider the modulus–threshold conflict. Mechanistic understanding of the modulus–threshold conflict has driven the development of polymers that resolve it.

1.5. Threshold is Amplified by Stress Deconcentration

All brittle materials concentrate stress alike; each fatigue-resistant material deconcentrates stress in its own way. How a material deconcentrates stress has rarely been studied historically, but has become a popular topic in recent years. Polymeric materials have a unifying feature: The physical interactions between chains are much weaker than the covalent bonds between repeat units along individual chains. This unifying feature enables polymeric materials to resist fatigue crack growth by deconcentrating stress. Here we review how stress deconcentrates in diverse polymeric materials, including polymer networks, particle-reinforced elastomers, glassy polymers, semicrystalline polymers, phase-separated polymers, and composites.

2. POLYMER NETWORKS

The Lake–Thomas model illustrates how stress deconcentrates in a polymer network and predicts its threshold (Section 1.4). This model has been tested experimentally in polymer networks of various architectures. Three examples are reviewed in this section.

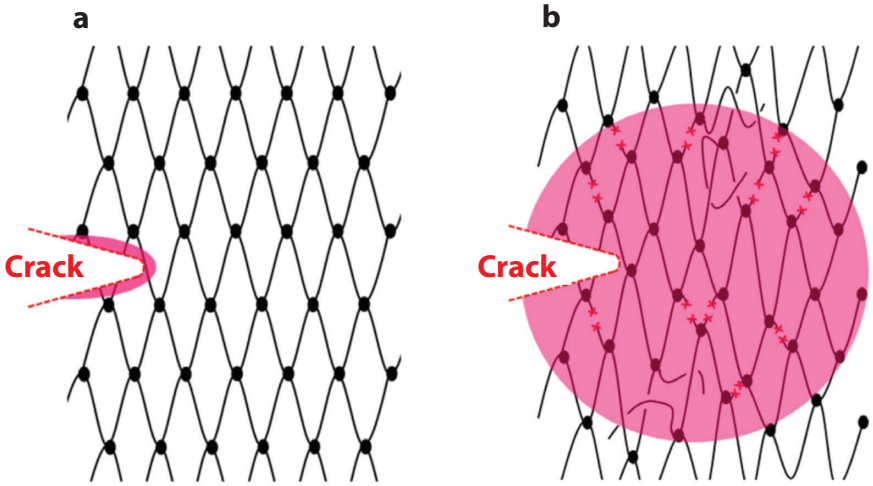

Figure 4

Unentangled polymer networks. (*a*) A perfect network fractures according to the Lake–Thomas model. (*b*) An imperfect network contains defects, and short chains break before long chains. Upon fracture, breaking chains off the crack plane dissipates energy. Such energy dissipation increases toughness but not threshold. Figure reproduced with permission from Reference 20; copyright 2019 Elsevier.

2.1. Unentangled Networks

The Lake–Thomas model assumes a perfect polymer network, in which all chains are of equal length, and no friction exists between chains (42). In such a perfect network, a crack grows by breaking polymer chains in a single layer, where chains off of the crack plane do not break (**Figure 4*a***). For the perfect network, toughness and threshold coincide—both are predicted by the Lake–Thomas model.

Most real polymer networks are imperfect, containing defects such as dangling chains, loops, and extremely long chains (**Figure 4*b***) (43, 44). Because polymer chains have distributed lengths, stress deconcentrates to chains both on and off the crack plane (45, 46). Chain scission occurs sequentially, distributed in a volume of the network around the crack tip. Distributed chain scission increases toughness but not threshold. For example, a PAAm hydrogel formed by radical polymerization has negligible interchain friction, but its threshold is one order of magnitude lower than its toughness (21, 35). This discrepancy is attributed to network imperfection, where distributed chain scission is indicated by the Mullins effect and a narrow, but nonzero, hysteresis loop (20, 47, 48).

These facts of real networks violate the assumptions of the Lake–Thomas model. Even so, setting the prefactor to one and averaging the chain length, the Lake–Thomas model approximates the threshold of imperfect networks. For a PAAm hydrogel, the threshold is measured to be 10 J/m^2 (20, 21). For a hydrogel of polymer volume fraction φ, the Lake–Thomas model becomes $G_{\text{th}} = \alpha\varphi n^{1/2} lJ/v$. Taking $\varphi = 10\%$, $v = 10^{-28}$ m^3, $n = 1{,}500$, $l = 4.6 \times 10^{-10}$ m, and $J = 5 \times 10^{-19}$ J, the Lake–Thomas model predicts a threshold of 8.9 J/m^2. Furthermore, long chains deconcentrate stress and lead to a high threshold—a PAAm hydrogel of long chains achieves a threshold of 250 J/m^2 (49).

Polymer networks can be synthesized with polymer chains of equal chain length, uniform composition, and few defects (**Figure 4*a***). One such polymer network is formed from tetra-arm poly(ethylene glycol) (tetra-PEG) (50). Swollen in water, such a polymer network has little interchain interaction and forms a hydrogel of negligible hysteresis (51). Because an ideal network is

nearly free of defects, polymer physics quantitatively models many of its mechanical properties (52). In a tetra-PEG hydrogel, the toughness and threshold coincide, and both are approximated by the Lake–Thomas model (53). Ideal networks thus suffer the modulus–threshold conflict. The threshold and modulus of ideal networks, approximately 10 J/m^2 and 10 kPa, respectively, are both lower than those required by many applications.

Recent simulations of an ideal network show that strain-stiffening causes stress to deconcentrate to polymer chains off the crack plane (54). For a PEG network, strain-stiffening increases the toughness by 30–40 times. Since the simulated networks are perfectly elastic, toughness and threshold coincide, and strain-stiffening also increases the threshold.

2.2. Entangled Networks

Many applications require polymer networks of both high modulus and high threshold. Modulus enables the networks to resist deformation, whereas threshold enables the networks to resist crack growth. However, modulus and threshold are both set by the number of repeat units per chain and thus form a trade-off relation: $E \propto {G_{\text{th}}}^{-1/2}$. Increasing chain length increases threshold, but decreases modulus.

The modulus–threshold conflict is resolved in a tanglemer: a polymer network in which entanglements greatly outnumber cross-links (55). Cross-links and entanglements play similar roles in setting the modulus of the network (**Figure 5*a***). Under small-to-modest deformation, no polymer chains break, and entanglements do not disentangle. For a tanglemer, entanglements greatly outnumber cross-links, and the modulus of the network scales as

$$E \propto 1/n_{\text{entangle}}, \qquad 5.$$

where n_{entangle} is the number of repeat units between neighboring entanglements along a polymer chain (38).

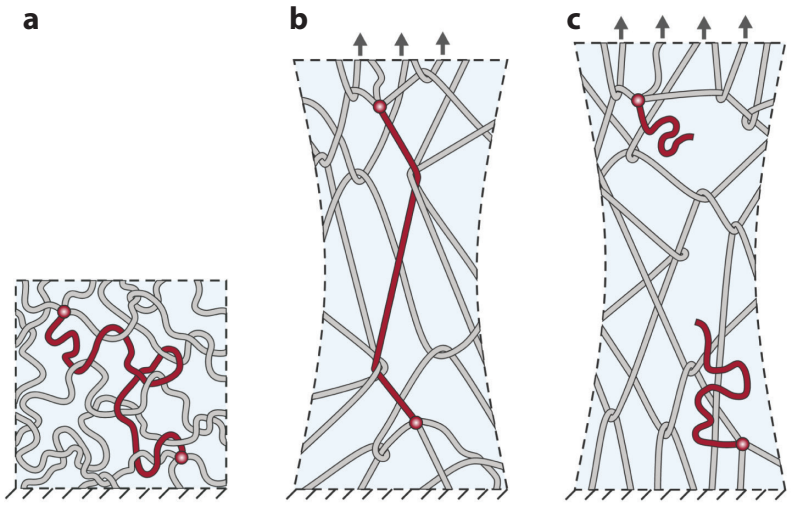

Figure 5

Highly entangled networks. (*a*) A tanglemer, a polymer network in which entanglements greatly outnumber cross-links. (*b*) When stretched, cross-links and entanglements constrain the motion of polymer chains, increasing the modulus. Tension deconcentrates along the entire length of each polymer chain. (*c*) When a polymer chain ruptures at a single covalent bond, the energy stored along the entire chain is released. Figure reproduced with permission from Reference 55; copyright 2021 AAAS.

By contrast, cross-links and entanglements play different roles in setting the threshold (55–57). Consider a polymer chain near rupture (the red chain in **Figure 5*b***). Where the chain meets a cross-link, the tension of the chain transmits through the cross-link to several other chains in the network. Consequently, the single chain bears higher tension than the other chains in the network. In this sense, cross-links concentrate stress. The chain may have many entanglements. When interchain friction is low, entanglements readily slip and do not impede the transmission of tension along the chain. When the polymer chain ruptures at a single covalent bond, the energy stored along the entire chain is released (**Figure 5*c***). In this sense, entanglements deconcentrate stress. Whereas dense cross-links reduce the threshold, dense entanglements do not. The threshold scales with the square root of chain length, which is set by cross-links and is unaffected by entanglements:

$$G_{\text{th}} \propto n^{1/2}. \qquad 6.$$

Tanglemers can be synthesized by polymerizing crowded monomers. Consider a hydrogel precursor of four molecular species: monomer, cross-linker, initiator, and water. Long polymer chains are created by reducing the cross-linker-to-monomer molar ratio, C. If the water-to-monomer molar ratio W is high, then monomers are sparse and polymerize into a sparsely entangled network. By contrast, if W is low, then monomers are crowded and polymerize into a highly entangled network. Submerged in water, the hydrogel swells, but the polymer network retains its connectivity, and entanglements do not disentangle.

In a tanglemer, dense entanglements set a high modulus, and long polymer chains set a high threshold. A fully swollen tanglemer PAAm hydrogel achieves a modulus of 100 kPa and a threshold of 200 J/m^2 (55). By contrast, a PAAm hydrogel of the same chain length and negligible entanglements swells enormously in water and has low modulus and threshold.

Many polymer networks are prepared by cross-linking preexisting polymer chains. This is primarily because certain polymers are not available in monomer form. Examples include polymers derived from natural sources, such as collagen, alginate, and chitosan (58, 59). Consider the specific example of polyethylene glycol (PEG). PEG is commonly synthesized by industrial processes. Without water, PEG is a semicrystalline polymer. In contact with water, PEG chains dissolve. To prevent dissolution or excessive swelling, PEG is often densely cross-linked into a network of short chains. Consequently, a PEG hydrogel is usually stiff and brittle, with a modulus of 675 kPa and a threshold less than 8 J/m^2 (57). Soft and tough PEG hydrogels can be prepared by fabricating a tanglemer from a dough. A PEG tanglemer hydrogel achieves a modulus of 55 kPa and a threshold of 100 J/m^2 at 93 wt% water (57).

Elastomers can be prepared with long chains and dense entanglements. In contrast to hydrogels, however, there is little or no solvent to lubricate the interactions between polymer chains. Furthermore, the entanglement density in an elastomer is set by the entanglement molecular weight, a thermodynamic property of the polymer (38). For example, polymerization with no solvent leads to a network of entanglement density approximately equal to that of the corresponding linear polymer melt (55, 60). Consequently, a tanglemer elastomer requires polymers of low interchain friction, such that tension transmits along polymer chains for long lengths, and low entanglement molecular weight, such that each polymer chain forms many entanglements. A tanglemer elastomer can be synthesized from monomers with a low cross-linker-to-monomer molar ratio C. For example, a poly(ethyl acrylate) (PEA) elastomer of long chains and dense entanglements achieves a modulus of 600 kPa and a threshold of 240 J/m^2 (55, 60). Without a large amount of solvent, preexisting polymers require intense mixing processes to incorporate cross-linkers and reagents, which break polymer chains (61). The resulting elastomers have short chains and thresholds on the order of 100 J/m^2. Recent work has synthesized elastomers from long, preexisting polymer chains using a combination of low-intensity kneading and annealing (62).

This work reported a polybutadiene tanglemer with a modulus of 800 kPa and a threshold of 440 J/m^2.

The notion of tanglemers has resonated with the lasting fascination with entanglements among polymer scientists (63). Can polymers be entangled by means other than thermal motion? Can polymers be entangled as densely as weaves and knits? Recent research entangles polymers by supramolecular templation (64).

2.3. Interpenetrating Networks

The modulus–threshold conflict is removed in double-network hydrogels (29). Interpenetrating polymer networks have been made using many different chemistries and architectures (11, 12, 65, 66). Consider a polyacrylamide/poly(2-acrylamido-2-methylpropane sulfonic acid) (PAAm/PAMPS) hydrogel (67). This hydrogel consists of a PAMPS network of short, stretched polymer chains (network A) interpenetrating with a PAAm network of long, relaxed polymer chains (network B).

The two polymer networks play different roles in setting the modulus and threshold of the hydrogel. Under a small stretch, the short chain network A bears the majority of the load. The modulus of the hydrogel scales as

$$E \propto 1/n_A, \qquad 7.$$

where n_A is the number of repeat units along a polymer chain in network A. Under a large stretch, network A ruptures, but network B survives. The hydrogel exhibits large hysteresis (65, 68). For the PAAm/PAMPS hydrogel, 90% of the PAMPS chains break before the gel ruptures (68). Hysteresis greatly increases the toughness but does not increase the threshold (31, 69). Loaded at the threshold, a crack advances by breaking chains in network B. The threshold scales as

$$G_{th} \propto {n_B}^{1/2}, \qquad 8.$$

where n_B is the number of repeat units along a polymer chain in network B. For a PAAm/PAMPS hydrogel, Equation 8 matches the scaling between threshold and chain length (39).

Long PAAm chains set a high threshold, whereas short PAMPS chains set a high modulus. A PAAm/PAMPS hydrogel achieves a threshold of 200 J/m^2 and a modulus of 400 kPa, both quantities being one order of magnitude larger than a single network PAAm hydrogel.

It is possible for the short chain network to contribute to the threshold. For example, considering only the contribution of the PAAm network, the threshold of PAAm/PAMPS hydrogels fits the Lake–Thomas model with a prefactor of six, rather than the usual two to three (31, 70). Similarly, a PEA/PEA double network elastomer achieves a threshold of 550 J/m^2, while the Lake–Thomas model predicts a threshold of ∼140 J/m^2 for a long chain network of $C = 10^{-4}$ (71). Moreover, for PEA/PEA elastomers loaded under threshold conditions, rupture of mechanofluorescent chains in the short chain network has been observed far from the crack plane (71, 72). While these interpenetrating networks have higher thresholds than the Lake–Thomas model predicts, the detailed reasons are unknown at present. It is plausible that the topology of interpenetrating networks can be designed to deconcentrate stress.

3. PARTICLE-REINFORCED POLYMER NETWORKS

Rubbers reinforced with rigid particles are used in high-volume applications, including tires, dampers, belts, and hoses (24). Adding particles to rubber amplifies various mechanical properties, including modulus, strength, and toughness. However, since fatigue crack growth in rubber was first characterized in the 1960s, it has been reported that adding particles does not markedly

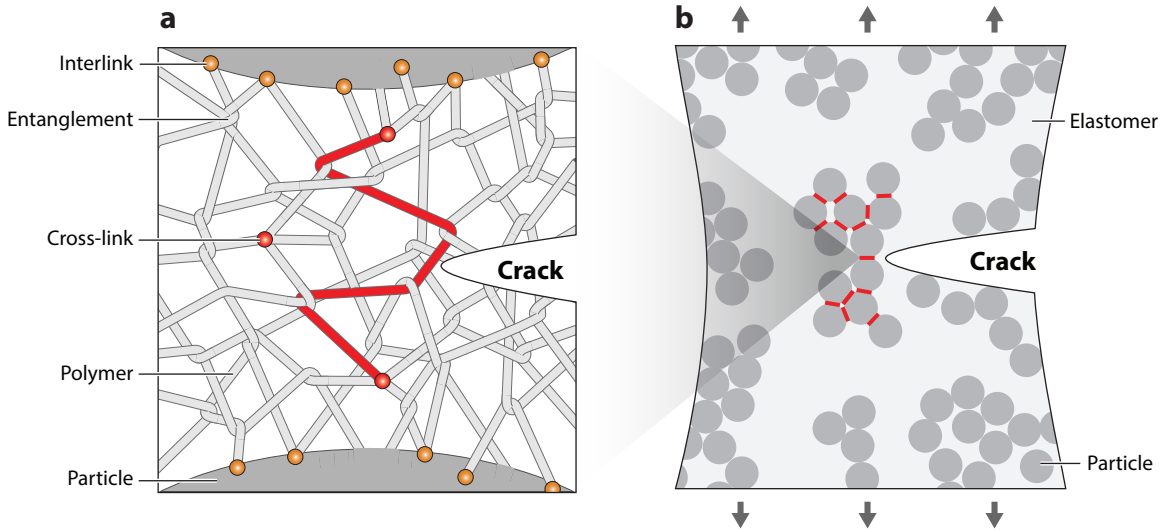

Figure 6

Multiscale stress deconcentration in a particle-reinforced tanglemer. (*a*) When a crack impinges on a polymer chain, rupture of a single bond along the chain dissipates the energy stored in all bonds along the chain. (*b*) When a crack impinges on a cluster of particles, rupture of a single particle–particle gap dissipates the energy stored in many particle–particle gaps in the cluster. Figure reproduced with permission from Reference 60; copyright 2023 The Author(s).

increase the threshold (4). For example, reinforcing natural rubber with carbon black increases its modulus by one-to-two orders of magnitude (24, 73, 74), but its threshold, reinforced or not, has remained approximately 100 J/m^2 for decades (4, 5, 28, 27). Similar observations have been made in particle-reinforced polymers of other chemistries, including, for example, carbon black–filled ethylene propylene diene monomer (EPDM) rubber, carbon black–filled styrene-butadiene rubber (SBR), and a silica-filled blend of 70% SBR and 30% butyl rubber (5, 29). All have thresholds between 50 and 100 J/m^2 for particle volume fractions ranging from 0.15 to 0.30.

Whether particles amplify the threshold was examined critically in a particle-reinforced tanglemer, in which polymer chains and rigid particles interlink by covalent bonds (60). Consider a crack impinging on a polymer chain (**Figure 6*a***). In a polymer network with low friction between polymer chains, stress deconcentrates along the entire polymer chain. Rupture of a single bond along the chain dissipates the energy stored in every bond along the chain. Next, consider a crack impinging on a particle cluster (**Figure 6*b***). Strong polymer–particle adhesion transmits high stress from polymers to particles. Because the particles are rigid, stress deconcentrates over many particle–particle gaps in the cluster. Rupture of a single gap dissipates energy stored in many gaps in the cluster. Consequently, stress deconcentrates over two length scales: polymers and particles. Long chains and clustered particles synergize across length scales to increase the threshold. A PEA network, with a cross-linker-to-monomer molar ratio of 10^{-4}, reinforced with silica nanoparticles at a particle-volume fraction of 0.45, achieves a threshold of 1,020 J/m^2.

If the polymer–particle adhesion is weak, then particles detach from polymers prior to crack growth, and the threshold is set by the matrix (60). The Lake–Thomas model applies, predicting a threshold of approximately 50 J/m^2. In a rubber reinforced with carbon particles, the polymer–particle adhesion is due to physical adsorption. Thresholds of several hundred Joules per square meter have been reported (5, 27, 30). The molecular mechanism for this enhancement has not been identified.

Particle-reinforced elastomers are typically synthesized from preexisting polymers, such as natural rubber, polybutadiene, and PDMS. Polymers and particles are commonly mixed with intense processes, which break polymer chains. As a result, polymer chains in particle-reinforced rubbers are typically short and densely cross-linked, with each chain containing 1,000 or fewer repeat units, leading to high moduli but low thresholds.

To meet this challenge, a particle-reinforced tanglemer is synthesized by mixing nanoparticles and liquid monomers, followed by polymerizing the monomers (60). Alternatively, a particle-reinforced tanglemer can be prepared from mixed emulsions (75). An aqueous emulsion of PEA and an aqueous emulsion of PMMA are prepared, such that both types of polymer chains are polymerized with silane coupling agents, and the two emulsions are mixed. When water evaporates, the PEA chains flow to form a space-filling matrix, and the PMMA particles remain rigid. The silane coupling agents condense to cross-link PEA chains and interlink PEA chains with the PMMA particles. A composite with 40% PMMA has a threshold greater than 1,000 J/m^2. The method of mixed emulsion divides labor between the emulsion maker and emulsion user. A facility with strict chemical control prepares an emulsion, and a user applies the emulsion without volatiles or high-intensity mixing processes. The method requires neither high-intensity mixing nor toxic monomers.

4. GLASSY POLYMERS

A polymer undergoes a glass transition at a temperature T_g. Examples of polymers that are glassy at room temperature include poly(methyl methacrylate) (PMMA) and polycarbonate (PC). A polymer glass may also undergo a ductile-to-brittle transition at a temperature T_{DB} (76, 77). At a temperature below T_{DB}, the stress–strain curve is nearly linear elastic up to fracture. At a temperature above T_{DB}, the stress–strain curve is elastic-plastic.

Experiments of crack growth in glassy polymers yield several observations. First, a brittle polymer glass has a lower toughness than a ductile polymer glass. At room temperature, PMMA is brittle and has a toughness of 300–1,000 J/m^2, whereas PC is ductile and has a toughness of 4,000–10,000 J/m^2 (22, 78). Second, the threshold of a glassy polymer is lower than its toughness: PMMA has a threshold of 15–45 J/m^2, and PC has a threshold of 25–65 J/m^2. Third, the ductile-to-brittle transition greatly affects toughness but has a smaller effect on threshold. The thresholds of various ductile and brittle polymer glasses fall in the range of 10–100 J/m^2 (**Figure 2*a***). Fourth, the thresholds of polymer glasses are higher than those of glasses such as silica, which has a threshold of ~1 J/m^2.

The Lake–Thomas model does not apply to glassy polymers for two reasons: Interchain friction is significant, and chains are not cross-linked. However, the notion of stress deconcentration still applies. In a polymer glass, the interchain friction is comparable to the yield strength of the material, on the order of 10 MPa. By contrast, the covalent strength between repeat units along a polymer chain is on the order of 10 GPa. It is this enormous difference between the interchain strength and intrachain strength that deconcentrates stress. For a polymer glass of short chains, a crack grows by chain slip without chain scission (**Figure 7*a***). For a polymer glass of long chains, a crack grows by a combination of chain slip and chain scission (**Figure 7*b***). We next sketch a model for the threshold of a polymer glass.

We estimate the length over which stress deconcentrates by applying the shear lag model to an individual polymer chain (56, 79). The model states that the stress applied to break a polymer chain, S_{chain}, is resisted by the shear stress applied along the length of the chain, $\tau_{interchain}$. The shear lag length, L, defines the length scale over which tension is transmitted from the chain to the matrix:

$$L = b\,(S_{chain}/\tau_{interchain}), \qquad 9.$$

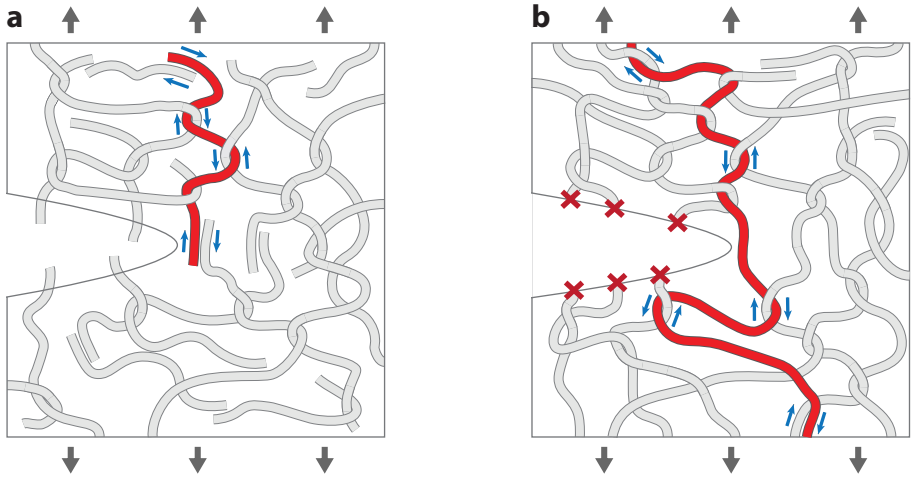

Figure 7

A crack impinges on a chain in a polymer glass. (*a*) For a polymer glass with short chains, a crack grows by chain slip. (*b*) For a polymer glass with long chains, a crack grows by a combination of chain slip and chain scission.

where b is the length per monomer. A chain shorter than the shear lag length will slip out at the crack plane. A chain longer than the shear lag length will fail by scission. Upon rupture, the polymer chain releases energy stored in tension. Consequently, the threshold scales with the covalent energy per unit area to rupture a layer of polymer strands of thickness $b(S_{\text{chain}}/\tau_{\text{interchain}})^{1/2}$:

$$G_{\text{th}} \propto (S_{\text{chain}}/\tau_{\text{interchain}})^{1/2} bJ/v. \quad 10.$$

In writing Equation 10, we assume that the undeformed polymer chain conforms to a random walk. Taking $S_{\text{chain}} = 10$ GPa, $\tau_{\text{interchain}} = 10$ MPa, and $b = 5 \times 10^{-10}$ m, the shear lag length is $L = 5 \times 10^{-7}$ m. Taking $J = 3.3 \times 10^{-19}$ J and $v = 4 \times 10^{-29}$ m^3, we predict the threshold of an non-cross-linked polymer glass to be 42 J/m^2. The interchain friction scales with the yield strength of the polymer glass, $\tau_{\text{interchain}} \propto \sigma_{\text{Y}}$. Consequently, Equation 10 implies a threshold–strength conflict:

$$G_{\text{th}} \propto {\sigma_{\text{Y}}}^{-1/2}. \quad 11.$$

Glassy polymers often have chains of over 10,000 repeat units, but shear lag limits stress deconcentration to 1,000 repeat units. Increasing interchain friction reduces the scale of stress deconcentration. At the limit of high interchain friction ($\tau_{\text{interchain}} \to S_{\text{chain}}$), the polymer glass behaves like silica. We note that interchain friction changes with both strain rate and viscosity. It has been shown that the toughness of a polymer network can increase as the interchain friction decreases by either high temperature or low strain rate (56). Similar effects were shown in a fiber composite where sliding is rate-sensitive (80).

This molecular picture is analogous to the microscopic picture of a fabric (81–83). Fabrics are composed of many fibers woven together. The fibers are strong, while the friction between fibers is low. Consequently, fibers slip before they break, deconcentrating stress. In particular, a solid glass is brittle, but a fabric of glass fibers is tough (84). The length scale of stress deconcentration is set by the shear lag model. If the fibers are knotted, then the length is bounded by the distance between knots. If a fiber in a fabric is not too long, a monotonic force can pull the fiber out without breaking it. The fiber can also be pulled out by a cyclic load of small amplitude (84). It is plausible that the cyclic force pulls the fiber out by ratcheting (85). It is also plausible that

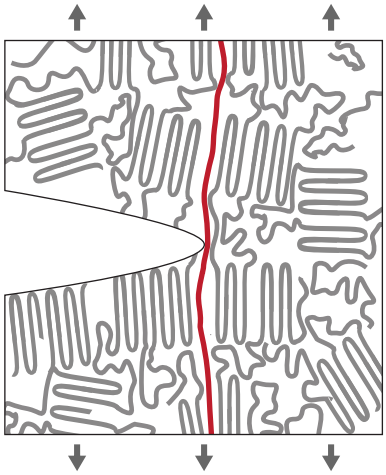

Figure 8

A crack impinges on a polymer chain in a semicrystalline polymer. The polymer consists of both crystalline and rubbery domains. Polymer chains are taken to be long enough to thread multiple crystalline domains.

ratcheting further deconcentrates stress over a long fiber. Although we make the analogy between fabrics and polymer glasses, ratcheting chain slip in polymer glasses has not been investigated.

5. SEMICRYSTALLINE POLYMERS

In a semicrystalline polymer, amorphous and crystalline domains coexist, ranging in size from nanometers to micrometers. The amorphous domains are rubbery at a temperature between the glass transition temperature and the melting temperature. In a high-molecular-weight polymer, the length of a chain can be larger than an individual crystalline domain, such that the chain can thread many crystalline domains. Such a chain is called a tie chain.

A crack grows by chain slip in a low-molecular-weight semicrystalline polymer and by a combination of chain slip and chain scission in a high-molecular-weight semicrystalline polymer. The transition has not been identified in the literature. Consider how stress deconcentrates at a crack tip in a high-molecular-weight semicrystalline polymer (**Figure 8**). Polymer chains are taken to be long enough to thread multiple crystalline domains. In both crystalline and rubbery domains, the physical interactions between chains are much weaker than the covalent bonds along an individual chain. In a rubbery domain, stress deconcentrates along the tie chain. In a crystalline domain, chains slip relative to each other, deconcentrating stress throughout the crystalline domain. Furthermore, adjacent crystalline domains are separated by thin layers of rubbery strands such that high tension can transmit over multiple crystalline domains. As the applied load cycles, crystalline domains rearrange, further deconcentrating stress at the crack tip. This multiscale stress deconcentration has not been studied. In the following sections, we describe data for several semicrystalline polymers.

5.1. Polyethylene

Polyethylene (PE) is classified by its density and molecular weight (86). Low-density PE (LDPE) has a density of 0.917–0.940 g/cm^3 and less than 1,500 repeat units per chain. High-density PE (HDPE) has a density of 0.941–0.965 g/cm^3 and approximately 5,000 repeat units per chain. Ultrahigh-molecular-weight PE has a density of 0.97 g/cm^3 and approximately 200,000 repeat

units per chain (87). For all these varieties, the glass transition temperature is approximately −110°C, and the melting temperature ranges from ∼105°C to ∼130°C (88). Consequently, at room temperature, PE consists of crystalline and rubbery domains. The volume fraction of crystalline domains (i.e., the crystallinity) ranges from 30% for LDPE to 80% for HDPE.

The toughness of HDPE ranges from 1,350 to 35,000 J/m^2 (22, 25, 26). The threshold of HDPE ranges from 35 J/m^2 to 340 J/m^2 (89). Furthermore, cross-links can reduce the length over which stress deconcentrates. For example, non-cross-linked HDPE has a threshold of 85 J/m^2, whereas highly cross-linked HDPE has a threshold of 51 J/m^2 (90). We are unable to identify a credible measurement for the threshold of LDPE. Much of the literature on PE reports toughness in terms of stress intensity factor K. We convert the data to energy release rate using the relation $G = K^2(1 - \nu^2)/E$, where we take the elastic modulus $E = 2$ GPa and Poisson's ratio $\nu = 0.4$.

5.2. Natural Rubber

Natural rubber is amorphous when undeformed but crystallizes when stretched. When rubber with a crack is stretched, strain concentrates near the crack tip, and chains crystallize near the crack tip but not elsewhere. Crystals resist crack growth, giving natural rubber an exceptionally high toughness of ∼10,000 J/m^2 while maintaining low hysteresis (24). However, the crystals melt when the strain is released and do not resist crack growth in cyclic loading. Natural rubber has a threshold of only ∼50 J/m^2 (14).

If natural rubber is only partially unloaded during each cycle, then the threshold can be much higher than 50 J/m^2 (8, 91, 92). For example, when each cycle reduces the load by one half, the measured threshold is over 1,000 J/m^2. Strain-induced crystals do not melt when the load is only partially relaxed, such that crystalline domains deconcentrate stress near the crack tip. Furthermore, strain-induced crystallization under nonrelaxing conditions causes the crack to deflect off of the crack plane, suggesting that crystallization is anisotropic (93). Applications can take advantage of this feature of natural rubber by operating in the stretched state (24).

Strain-induced crystallization occurs in elastomers other than natural rubber. Classic examples include neoprene and polyisoprene (24). Recently, a PEG hydrogel with slide-ring cross-links that crystallizes when stretched was synthesized (94). As a second example, a PEG hydrogel formed by end-linking and deswelling star polymers achieves strain-induced crystallinity of up to 50% (95). Fatigue crack growth has not been studied in these materials.

5.3. Thermoplastic Polyurethane

Thermoplastic polyurethanes (TPU) are block copolymers with alternating blocks of soft and hard segments. The soft and hard segments phase-separate into soft and hard domains. The hard domains are discontinuous such that the material is stretchable. The hard domains can be either amorphous or crystalline and typically have dimensions of tens of nanometers. TPU is thus a nanocomposite of two phases, where hard domains serve as multifunctional cross-links and reinforcing particles. Since the hard domains melt at high temperatures, TPU can be molded and reformed, similar to thermoplastics and metals. Furthermore, the phase-separated structure of TPU leads to superior mechanical properties, such as high modulus, high strength, and wear resistance.

Hard domains in TPU fragment under a large stretch (96). The fragmentation of hard domains correlates with strain-stiffening, which persists in cyclic loading. Depending on its chemistry, TPU can be crystalline as prepared or it can crystallize under a large stretch. In strain-crystallizing TPU, the strain-induced crystals are partially retained after the stretch is removed. Both semicrystalline TPU and strain-crystallizing TPU have high thresholds, ranging from 500 to 2,500 J/m^2

(32–34). In fatigue crack growth, strain concentrates near the crack tip, locally fragmenting the hard domains and crystallizing TPU (34). The material near the crack tip is thus selectively reinforced to resist crack growth in future cycles, leading to a high threshold.

5.4. Poly(Vinyl Alcohol) Hydrogels

Poly(vinyl alcohol) (PVA) hydrogels are semicrystalline (97, 98). Methods to achieve high crystallinity include freeze–thaw, salting out, and annealing (99, 100). PVA hydrogels are commonly non-cross-linked. In a high-molecular-weight PVA hydrogel, a crack grows by a combination of chain slip and chain scission. Crystalline domains deconcentrate stress near a crack tip, and the threshold increases with the degree of crystallinity (101). At 20 wt% crystallinity, the threshold can exceed 1,000 J/m^2.

The threshold is also increased by aligning crystalline domains. Methods to align crystalline domains include applying a stretch during salting out (102), mechanical training after crystallization (103), and directional freezing (104). These techniques elongate the crystalline domains in one direction and form fibrils composed of many crystalline domains. For example, mechanical training forms crystalline fibrils of PVA, approximately 1 μm in diameter (103). In front of a crack, stiff fibrils deconcentrate stress over long distances, increasing the threshold. Such hydrogels achieve thresholds greater than 1,000 J/m^2 at a crystallinity of only 2.8 wt%, compared with 20 wt% without training. Furthermore, the threshold is anisotropic, reaching a minimum in the direction parallel to training. At higher volume fractions, the difference between the threshold in the parallel and perpendicular directions varies enough for a crack to deflect toward the brittle direction (102, 104). If a fatigue crack kinks during a test, then the threshold in the original direction of the crack can no longer be measured.

6. PHASE-SEPARATED POLYMERS

Mixtures of different species of polymers tend to separate into phases. The phases can be bicontinuous, or one phase can be dispersed in the other (105). Without a mechanism to halt their growth, the phases will coarsen with time. Phase coarsening requires that polymer chains be mobile, and it can be arrested by various mechanisms that immobilize polymer chains. For example, when polymer chains of at least one species cross-link into a network, the network prevents polymer chains from migrating over long distances and thereby arrests phase coarsening. As a second example, species of polymer chains can be mobile at an elevated temperature but become immobile by crystallization or vitrification as the temperature drops (106–110). As a third example, a block copolymer can form rubbery and glassy domains, which immobilize polymers and arrest phase coarsening (111, 112).

Phase-separated polymers can have high thresholds. For example, consider a poly(methyl methacrylate)–poly(acrylic acid) (PMMA–PAAc) hydrogel (113). PMMA is a glass-forming polymer, whereas PAAc is a hydrogel-forming polymer. To mix these polymers, a PMMA plastic is swollen in an AAc monomer and a small amount of water. Upon polymerization of the AAc monomer, the polymers separate into a hydrogel phase and a glass phase. The two phases arrest at the nanoscale and are bicontinuous. The thermodynamics and ternary phase diagram of this system have been recently studied (114). The phase diagram fits a modified Flory–Huggins model, where amphiphilic AAc monomers bridge hydrophobic PMMA polymers and water. The nanocomposite hydrogel has a threshold greater than 1,000 J/m^2. By contrast, PMMA has a threshold of 50 J/m^2, and the pure PAAc hydrogel has a threshold of 150 J/m^2.

The molecular mechanism for the high threshold of such a material has been obscure. Under monotonic loading, bulk PMMA is brittle and ruptures at a strain of 5%. Inelastic deformation is

localized near the fracture plane, where PMMA fractures by a combination of slip and scission of polymer chains. Chain slip leads to bands of nanoscale fibrils, called crazes (115). Fracture takes place by the propagation of a single band of fibrils. Even though individual fibrils undergo large plastic strain, the rupture strain of bulk PMMA is small. Brittle glassy polymers can be ductile at the nanoscale (116, 117). For example, a freestanding PS polymer film, 250 nm thick, showed a rupture strain of ~200%, two orders of magnitude greater than that of the bulk polymer (118). Ductile behavior has also been demonstrated in a nanocomposite of PMMA and PEA (119). Therefore, it is conceivable that nanoscale PMMA phases in a PMMA–PAAc hydrogel undergo plastic deformation prior to rupture. Plastic deformation may rearrange PMMA phases to deconcentrate stress in cyclic loading. As of this writing, no systematic study of fatigue crack growth in a glass–hydrogel nanocomposite can be identified.

The thresholds of phase-separated polymers vary considerably with the polymers' chemistry and structure. SBR and natural rubber blends have thresholds of 200 J/m^2, higher than either polymer alone (27). Thermoplastic elastomers of cross-linked EPDM rubber particles dispersed in a polypropylene matrix have thresholds of 1,000 J/m^2 (24, 120). Self-healing polyampholyte hydrogels with bicontinuous hard and soft phases have thresholds of 100 J/m^2 (121, 122). A double-network elastomer, in which the first network is formed from the copolymerization of 2-methoxyethyl acrylate (MEA) and PAMPS and the second network is MEA, phase-separates into phases rich or poor in PAMPS (123). Both phases are rubbery at room temperature, and the resulting elastomer has a threshold of 500 J/m^2. Recently, a hydrogel of PEA–PAAc was synthesized with superior strength and negligible hysteresis (124). Both phases were rubbery at room temperature, and the threshold was comparable to that of the dry PEA network, 150 J/m^2. Lastly, a fatigue-resistant polymer electrolyte was created from an interpenetrating network of a plastic electrolyte and a rubber, increasing the threshold by 175% (125). In many cases, the materials consist of both hard and soft phases. It is possible that the hard phase deconcentrates stress near a crack tip, increasing the threshold. Hopefully, research will soon elucidate the mechanism of stress deconcentration in phase-separated polymers.

7. COMPOSITES

Composites are made by embedding polymer matrices with stiff fibers (126–128). The fibers bear high loads, and the matrices bind the fibers into continuous materials. Polymer matrix composites gained attention soon after polymer industries emerged in the 1930s. Today, polymer matrix composites are used in many high-volume applications, including lightweight, stiff, and strong materials for aerospace structures (129, 130) and elastomers reinforced with steel wires and plastic threads for belts and tires (24). The last decade has seen the development of fiber-reinforced hydrogels for health care (131–137).

Composites suffer fatigue crack growth. Consider a crack impinging on a fiber. The fibers are much stiffer than the matrix, and the adhesion between fiber and matrix is strong. At the crack tip, the soft matrix shears greatly, allowing high stress to transmit along a segment of the fiber. When the fiber ruptures, all of the elastic energy stored in the stressed segment is released. This deconcentration of stress increases the toughness of the composite. If the deformation is elastic, then this stress deconcentration also increases the threshold. This mechanism differs from that in composites of ceramic fibers and ceramic matrices, in which fibers and the matrix have similar elastic moduli, and the fiber–matrix interfaces are designed to have weak adhesion (37). During fracture, after the matrix cracks, weak adhesion enables the fibers to slide relative to the matrix and distribute high stress over segments of the fibers.

In a composite of glass or carbon fibers embedded in a polymer matrix, fibers and the matrix have a large difference in elastic moduli. The high modulus contrast promotes stress

deconcentration. However, little data exist for fatigue crack growth in the direction perpendicular to the fibers (138, 139). This is perhaps due to the high resistance to crack growth in this direction, which leads to crack kinking, distributed damage, and interlaminar delamination. By contrast, fatigue crack growth through the matrix between fibers is well studied (139–142). Adding fibers that bridge the interface between plies, called z-pins, increases the interlaminar threshold of a carbon fiber composite from 200 J/m^2 to 2,000 J/m^2 (143).

A fiber composite can be made stretchable by using stretchable fibers (144, 145). For example, a composite of stiff PDMS fibers embedded in a soft PDMS matrix achieves a stretch of two prior to rupture (145). The PDMS composite achieves a threshold of 170 J/m^2. A composite of PDMS fibers embedded in a hydrogel matrix achieves a threshold of 1,000 J/m^2 (23). Similarly, a composite of spandex fibers embedded in a polyurethane matrix achieves a threshold of 3,900 J/m^2 (146). In these composites, the threshold scales with the fiber diameter, and the scaling factor increases as the modulus ratio increases. We note that the scale of stress deconcentration potentially exceeds the sample size, making the measured threshold depend on the sample size. If it does, increasing the sample size will increase the measured threshold until the sample is large enough for stress deconcentration to be localized near the crack tip. The condition where the scale of stress deconcentration exceeds the sample size is analogous to the condition of large-scale bridging under monotonic loading (147).

Fibers deconcentrate stress only near cracks growing perpendicular to the fibers. To deconcentrate stress in multiple directions, a stiff and stretchable lattice can be embedded in a soft matrix (148). Near a crack impinging on one segment of the lattice, stress deconcentrates along the length of the segment. A square lattice of stiff elastomer embedded in a soft elastomer matrix deflects a crack with $G = 537$ J/m^2 (148). Stiff lattices are analogous to mechanical metamaterials, where the toughness scales with the square root of the strut length (149, 150). Strain-stiffening struts can further deconcentrate stress (54). Biological tissues often contain stiff fibers in soft matrices and can achieve high thresholds (151).

8. LENGTH SCALE OF STRESS DECONCENTRATION

8.1. Cyclically Stretch a Sample Without a Precut Crack

The bulk of this review focuses on an experiment that cyclically loads a sample with a precut crack (**Figure 1**). Another type of experiment is also commonly run in which a sample without a precut crack is cyclically loaded (**Figure 9*a***). For example, the applied stress is cycled between zero and an amplitude S, and the number of cycles to rupture N is recorded (**Figure 9*b***). The outcome of this experiment is plotted as a point on the S–N plane (**Figure 9*c***). The outcome is statistical—that is, another sample cycled with the same amplitude of stress S will rupture after a different number of cycles, producing a different point on the S–N plane. To obtain a statistically significant dataset, the experiment is run at the same amplitude of stress for many samples.

When the amplitude of stress is large, a sample may rupture while the stress is monotonically increasing in the first cycle. This run of the experiment measures the strength of the material S_c, and is plotted as an open circle in the S–N plane. The strength of the material will vary from sample to sample and result in a set of data points. From this set of data points, one may report the average and standard deviation of the strength. A large number of samples must be tested to determine the strength with a low quantile of rupture (152). High-throughput experiments have been designed for testing many samples simultaneously (153, 154).

The repeated runs of this experiment result in a dataset—a cloud of data points on the S–N plane. By connecting representative data points, the experimentalist may report an S–N curve. Such an S–N curve is commonly quoted, but should be used with caution. The outcomes of the experiment are statistical and result in an S–N cloud.

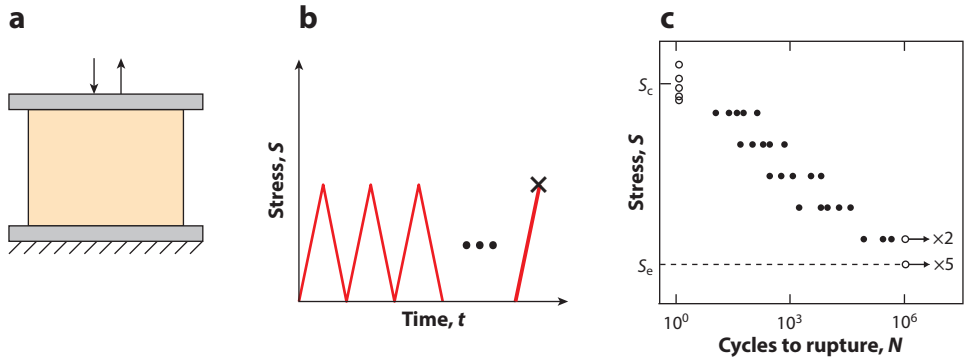

Figure 9

Cyclically stretching a sample without a precut crack. (*a*) A sample with no precut crack is cyclically stretched. (*b*) The applied stress cycles between zero and an amplitude S. After a number of cycles N, the sample ruptures. (*c*) The results of many tests are plotted on the S–N plane. The experiment is terminated after a designated number of cycles. An open circle represents a sample that ruptures under monotonic loading. A solid point represents a sample that ruptures after some cycles of load. An open circle with an arrow represents a sample that does not rupture after the designated number of cycles.

The endurance limit is the amplitude of stress below which the material can survive an infinite number of cycles. This definition, however, is not experimentally operational. In practice, the experimentalist designates a finite number of cycles at which to terminate the experiment. At a given amplitude of stress, a sample either ruptures before the designated number of cycles or survives the designated number of cycles. On the S–N plane, the former is marked by a solid point, and the latter is marked by an open circle with an arrow. The experimentalist also designates a finite number of samples to test at each amplitude of stress. The endurance limit is set to be the highest amplitude of stress at which all samples survive. This practical definition clearly depends on the designated number of cycles as well as the designated number of samples to test at each amplitude of stress. The literature is evasive about these practical difficulties. Thus, one should be cautious about any reported values of endurance limit. This challenge is general for estimating any statistic from a dataset (154).

When a sample without a precut crack is cyclically loaded, the endurance work W_e is defined as the strain energy density below which the material can be stretched for an infinite number of cycles (155). Like threshold, W_e is a material property. For the purposes of this discussion, we use W_e only in scaling relations and thus neglect any differences in W_e due to the type of loading, such as uniaxial tension and biaxial tension.

8.2. Endurance Fractocohesive Length

The ratio of G_{th} to W_e produces a length scale, G_{th}/W_e, called the endurance fractocohesive length (69). This length scales the zone of material near a crack that elastically deforms when the material is loaded at the threshold. The endurance fractocohesive length thus provides the scale of stress deconcentration. For linear elastic materials, the endurance fractocohesive length reduces to $2K_{th}^2/S_e^2$, where K_{th} is the threshold stress intensity factor and S_e is the endurance strength. Values of this length are collected in Reference 22.

The endurance fractocohesive length scales the flaw sensitivity length in fatigue loading. For materials under cyclic loading, if the initial flaw size is larger than this length, then the material's resistance to rupture is characterized by the threshold G_{th}. By contrast, if the initial flaw size is smaller than this length, then the material's resistance to rupture is characterized by the

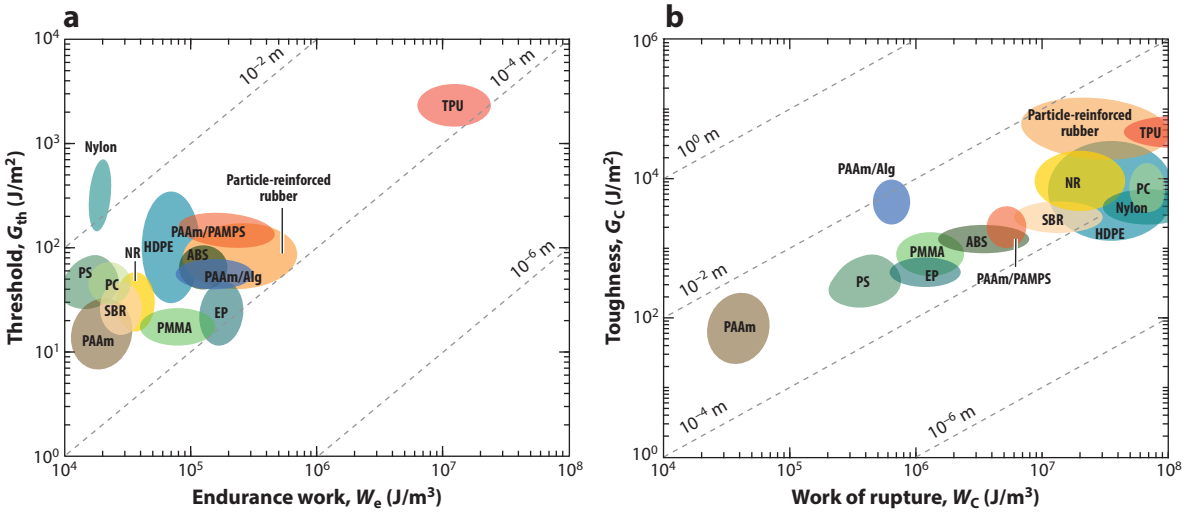

Figure 10

Scale of stress deconcentration. (*a*) Various polymers plotted on the plane of endurance work W_e and threshold G_{th}. Lines of constant endurance fractocohesive length G_{th}/W_e are plotted along the diagonal. (*b*) Various materials plotted on the plane of toughness G_c and work of rupture W_c. Lines of constant fractocohesive length G_c/W_c are plotted along the diagonal. Data for nylon from References 22, 157, and 158. Data for polystyrene (PS), poly(methyl methacrylate) (PMMA), and epoxy (EP) from References 22 and 157. Data for polycarbonate (PC) from References 22, 159, and 160. Data for styrene-butadiene rubber (SBR) from References 22 and 161). Data for high-density polyethylene (HDPE) from References 22, 25, 26, and 162. Data for acrylonitrile butadiene styrene (ABS) from References 22, 163, and 164. Data for natural rubber (NR) from References 9, 22, 61, and 157. Data for particle-reinforced rubber from References 4, 5, 22, 24, 27, 28, 73, 74, and 157. Data for polyacrylamide/poly(2-acrylamido-2-methylpropanesulfonic acid) (PAAm/PAMPS) from Reference 67. Data for thermoplastic polyurethane (TPU) from References 32–34. Data for polyacrylamide (PAAm) from References 21, 35, and 157. Data for polyacrylamide/alginate (PAAm/Alg) from References 18 and 19.

endurance work W_e. Data for polymers are plotted on the plane of threshold and endurance work, where the endurance fractocohesive length is indicated by the diagonal dashed lines (**Figure 10*a***). For stiff materials, we calculate the endurance work using linear elasticity as $W_e = S_e^2/2E$. For stretchable materials, we calculate endurance work as the area under the stress–strain curve in steady-state loading. In defining the threshold and endurance work, we assume cracks are either long or negligible, respectively (156).

The endurance fractocohesive length, G_{th}/W_e, can be compared with its analog in monotonic loading. For a material with a long crack subject to a monotonic load, the resistance to crack growth is characterized by the toughness G_c. For a material without a long crack, the work of rupture W_c is defined as the strain energy density at rupture under monotonic loading. The ratio of G_c to W_c produces a length scale, G_c/W_c, called the fractocohesive length or flaw sensitivity length (157). The length G_c/W_c scales the size of the fracture process zone in monotonic loading. The physics of G_{th}/W_e is different from G_c/W_c, since threshold does not include inelastic processes. For a given material, G_c/W_c and G_{th}/W_e are two distinct material properties. Data for polymers are plotted on the plane of toughness and work of rupture, where the fractocohesive length is indicated by diagonal dashed lines (**Figure 10*b***). Most polymers have both G_c/W_c and G_{th}/W_e between 10^{-4} and 10^{-2} m. In general, the two lengths are uncorrelated.

9. CONCLUDING REMARKS

Polymeric materials have a unifying feature: The physical interactions between chains are much weaker than the covalent bonds between repeat units along individual chains. This unifying feature

enables polymeric materials to resist fatigue crack growth by deconcentrating stress. We describe how stress deconcentrates in diverse polymeric materials, including polymer networks, particle-reinforced elastomers, glassy polymers, semicrystalline polymers, phase-separated polymers, and composites. How stress deconcentration amplifies threshold has been extensively studied in elastomers and gels but has received much less attention in glassy and semicrystalline polymers. Also, few studies exist for thresholds in phase-separated polymers and composites. Recent years have seen significant advances in the understanding of molecular processes to amplify the threshold through stress deconcentration at the crack tip. By contrast, molecular processes of the endurance limit of samples without precut cracks have remained obscure. Furthermore, ample opportunities exist for fatigue-resistant adhesives and biopolymers.

DISCLOSURE STATEMENT

The authors are not aware of any affiliations, memberships, funding, or financial holdings that might be perceived as affecting the objectivity of this review.

ACKNOWLEDGMENTS

This was supported by the National Science Foundation (NSF) through the Harvard University Materials Research Science and Engineering Center DMR-2011754 and by the Air Force Office of Scientific Research under award number FA9550-20-1-0397. J.S. and C.H.A. were supported by NSF Graduate Research Fellowships (grant DGE1745303).

LITERATURE CITED

1. Thomas AG. 1958. Rupture of rubber. V. Cut growth in natural rubber vulcanizates. *J. Polym. Sci.* 31:467–80
2. Rivlin RS, Thomas AG. 1953. Rupture of rubber. I. Characteristic energy for tearing. *J. Polym. Sci.* 10:291–318
3. Paris PC, Gomez MP, Anderson WE. 1961. A rational analytic theory of fatigue. *Trend Eng.* 13:9–14
4. Lake GJ, Lindley PB. 1965. The mechanical fatigue limit for rubber. *J. Appl. Polym. Sci.* 9:1233–51
5. Heinrich G, Kipscholl R, Stoček R, eds. 2021. *Fatigue Crack Growth in Rubber Materials: Experiments and Modelling*. Cham, Switz.: Springer Int. Publ.
6. Bai R, Yang J, Suo Z. 2019. Fatigue of hydrogels. *Eur. J. Mech. A/Solids* 74:337–70
7. Lake GJ, Lindley PB. 1964. Cut growth and fatigue of rubbers. II. Experiments on a noncrystallizing rubber. *J. Appl. Polym. Sci.* 8:707–21
8. Lindley PB. 1973. Relation between hysteresis and the dynamic crack growth resistance of natural rubber. *Int. J. Fract.* 9:449–62
9. Lake GJ. 1995. Fatigue and fracture of elastomers. *Rubber Chem. Technol.* 68:435–60
10. Mars WV, Fatemi A. 2004. Factors that affect the fatigue life of rubber: a literature survey. *Rubber Chem. Technol.* 77:391–412
11. Zhao X. 2014. Multi-scale multi-mechanism design of tough hydrogels: building dissipation into stretchy networks. *Soft Matter* 10:672–87
12. Zhao X, Chen X, Yuk H, Lin S, Liu X, Parada G. 2021. Soft materials by design: unconventional polymer networks give extreme properties. *Chem. Rev.* 121:4309–72
13. Gehling T, Schieppati J, Balasooriya W, Kerschbaumer RC, Pinter G. 2023. Fatigue behavior of elastomeric components: a review of the key factors of rubber formulation, manufacturing, and service conditions. *Polym. Rev.* 63:763–804
14. Lake GJ, Thomas AG. 1967. The strength of highly elastic materials. *Proc. R. Soc. A* 300:108–19
15. Gent AN, Tobias RH. 1982. Threshold tear strength of elastomers. *J. Polym. Sci. Polym. Phys. Ed.* 20:2051–58

16. Mueller HK, Knauss WG. 1971. The fracture energy and some mechanical properties of a polyurethane elastomer. *Trans. Soc. Rheol.* 15:217–33
17. Bhowmick AK. 1988. Threshold fracture of elastomers. *J. Macromol. Sci. C* 28:339–70
18. Sun JY, Zhao X, Illeperuma WRK, Chaudhuri O, Oh KH, et al. 2012. Highly stretchable and tough hydrogels. *Nature* 489:133–36
19. Bai R, Yang Q, Tang J, Morelle XP, Vlassak J, Suo Z. 2017. Fatigue fracture of tough hydrogels. *Extreme Mech. Lett.* 15:91–96
20. Canhui Y, Tenghao Y, Zhigang S. 2019. Polyacrylamide hydrogels. I. Network imperfection. *J. Mech. Phys. Solids* 131:43–55
21. Zhang E, Bai R, Morelle XP, Suo Z. 2018. Fatigue fracture of nearly elastic hydrogels. *Soft Matter* 14:3563–71
22. Fleck NA, Kang KJ, Ashby MF. 1994. Overview no. 112: the cyclic properties of engineering materials. *Acta Metall. Mater.* 42:365–81
23. Xiang C, Wang Z, Yang C, Yao X, Wang Y, Suo Z. 2019. Stretchable and fatigue-resistant materials. *Mater. Today* 30:7–16
24. Gent AN. 2012. *Engineering with Rubber: How to Design Rubber Components*. Munich: Hansen Publ. 3rd ed.
25. Chan MKV, Williams JG. 1981. Plane strain fracture toughness testing of high density polyethylene. *Polym. Eng. Sci.* 21:1019–26
26. Kwon HJ, Jar P-YB. 2006. Toughness of high-density polyethylene in plane-strain fracture. *Polym. Eng. Sci.* 46:1428–32
27. Robertson CG, Stoček R, Kipscholl C, Mars WV. 2019. Characterizing the intrinsic strength (fatigue threshold) of natural rubber/butadiene rubber blends. *Tire Sci. Technol.* 47:292–307
28. Gent AN, Lai S-M, Nah C, Wang C. 1994. Viscoelastic effects in cutting and tearing rubber. *Rubber Chem. Technol.* 67:610–18
29. Lake GJ. 1972. Mechanical fatigue of rubber. *Rubber Chem. Technol.* 45:309–28
30. Mzabi S, Berghezan D, Roux S, Hild F, Creton C. 2011. A critical local energy release rate criterion for fatigue fracture of elastomers. *J. Polym. Sci. B* 49:1518–24
31. Zhang W, Liu X, Wang J, Tang J, Hu J, et al. 2018. Fatigue of double-network hydrogels. *Eng. Fract. Mech.* 187:74–93
32. Major Z. 2020. Methodology used for characterizing the fracture and fatigue behavior of thermoplastic elastomers. In *Fatigue Crack Growth in Rubber Materials*, ed. G Heinrich, R Kipscholl, R Stoček, pp. 273–96. Cham, Switz.: Springer Int. Publ.
33. Scetta G, Selles N, Heuillet P, Ciccotti M, Creton C. 2021. Cyclic fatigue failure of TPU using a crack propagation approach. *Polym. Test.* 97:107140
34. Scetta G, Euchler E, Ju J, Selles N, Heuillet P, et al. 2021. Self-organization at the crack tip of fatigue-resistant thermoplastic polyurethane elastomers. *Macromolecules* 54:8726–37
35. Tang J, Li J, Vlassak JJ, Suo Z. 2017. Fatigue fracture of hydrogels. *Extreme Mech. Lett.* 10:24–31
36. Griffith AA. 1921. The phenomena of rupture and flow in solids. *Philos. Trans. R. Soc. A* 221:163–98
37. Ritchie RO, Dauskardt RH. 1991. Cyclic fatigue of ceramics: a fracture mechanics approach to subcritical crack growth and life prediction. *J. Ceram. Soc. Jpn.* 99:1047–62
38. Rubinstein M, Colby RH. 2003. *Polymer Physics*. Oxford, NY: Oxford Univ. Press
39. Zhou Y, Zhang W, Hu J, Tang J, Jin C, et al. 2020. The stiffness-threshold conflict in polymer networks and a resolution. *J. Appl. Mech.* 87:031002
40. Ashby MF. 2005. *Materials Selection in Mechanical Design*. Amsterdam: Butterworth-Heinemann. 3rd ed.
41. Ritchie RO. 2011. The conflicts between strength and toughness. *Nat. Mater.* 10:817–22
42. Mao Y, Talamini B, Anand L. 2017. Rupture of polymers by chain scission. *Extreme Mech. Lett.* 13:17–24
43. Kim J, Yin T, Suo Z. 2022. Polyacrylamide hydrogels. V. Some strands in a polymer network bear loads, but all strands contribute to swelling. *J. Mech. Phys. Solids* 168:105017
44. Gu Y, Zhao J, Johnson JA. 2019. A (macro)molecular-level understanding of polymer network topology. *Trends Chem.* 1:318–34
45. Tehrani M, Sarvestani A. 2017. Effect of chain length distribution on mechanical behavior of polymeric networks. *Eur. Polym. J.* 87:136–46

46. Vernerey FJ, Brighenti R, Long R, Shen T. 2018. Statistical damage mechanics of polymer networks. *Macromolecules* 51:6609–22
47. Mullins L. 1948. Effect of stretching on the properties of rubber. *Rubber Chem. Technol.* 21:281–300
48. Diani J, Fayolle B, Gilormini P. 2009. A review on the Mullins effect. *Eur. Polym. J.* 45:601–12
49. Zhang W, Gao Y, Yang H, Suo Z, Lu T. 2020. Fatigue-resistant adhesion I. Long-chain polymers as elastic dissipaters. *Extreme Mech. Lett.* 39:100813
50. Sakai T, Matsunaga T, Yamamoto Y, Ito C, Yoshida R, et al. 2008. Design and fabrication of a high-strength hydrogel with ideally homogeneous network structure from tetrahedron-like macromonomers. *Macromolecules* 41:5379–84
51. Sakai T, Akagi Y, Matsunaga T, Kurakazu M, Chung U, Shibayama M. 2010. Highly elastic and deformable hydrogel formed from tetra-arm polymers. *Macromol. Rapid Commun.* 31:1954–59
52. Sakai T, ed. 2020. *Physics of Polymer Gels*. Weinheim, Ger.: Wiley-VCH
53. Lin S, Ni J, Zheng D, Zhao X. 2021. Fracture and fatigue of ideal polymer networks. *Extreme Mech. Lett.* 48:101399
54. Deng B, Wang S, Hartquist C, Zhao X. 2023. Nonlocal intrinsic fracture energy of polymerlike networks. *Phys. Rev. Lett.* 131:228102
55. Kim J, Zhang G, Shi M, Suo Z. 2021. Fracture, fatigue, and friction of polymers in which entanglements greatly outnumber cross-links. *Science* 374:212–16
56. Hassan S, Kim J, Suo Z. 2022. Polyacrylamide hydrogels. IV. Near-perfect elasticity and rate-dependent toughness. *J. Mech. Phys. Solids* 158:104675
57. Nian G, Kim J, Bao X, Suo Z. 2022. Making highly elastic and tough hydrogels from doughs. *Adv. Mater.* 34:2206577
58. Licup AJ, Münster S, Sharma A, Sheinman M, Jawerth LM, et al. 2015. Stress controls the mechanics of collagen networks. *PNAS* 112:9573–78
59. Kohjiya S, Ikeda Y, eds. 2021. *Chemistry, Manufacture, and Applications of Natural Rubber*. Duxford, UK: Woodhead Publ. 2nd ed.
60. Steck J, Kim J, Kutsovsky Y, Suo Z. 2023. Multiscale stress deconcentration amplifies fatigue resistance of rubber. *Nature* 624:303–8
61. Pike M, Watson WF. 1952. Mastication of rubber, I. Mechanism of plasticizing by cold mastication. *J. Polym. Sci.* 9:229–51
62. Bao X, Nian G, Kutsovsky Y, Kim J, Jiao Q, Suo Z. 2023. Low-intensity mixing process of high molecular weight polymer chains leads to elastomers of long network strands and high fatigue threshold. *Soft Matter* 19:5956–66
63. Wang F-S, Kosovsky LM, Krist EC, Kruse BJ, Zhukhovitskiy AV. 2024. Trapped entanglements in polymer networks: formation and characterization. *Trends Chem.* 6:447–58
64. Krist EC, Kruse BJ, Dickenson JC, Zhukhovitskiy AV. 2024. Supramolecular templation of entanglements in organogels. *Macromolecules* 57:7878–83
65. Gong JP. 2010. Why are double network hydrogels so tough? *Soft Matter* 6:2583–90
66. Chen Q, Chen H, Zhu L, Zheng J. 2015. Fundamentals of double network hydrogels. *J. Mater. Chem. B* 3:3654–76
67. Gong JP, Katsuyama Y, Kurokawa T, Osada Y. 2003. Double-network hydrogels with extremely high mechanical strength. *Adv. Mater.* 15:1155–58
68. Nakajima T, Kurokawa T, Ahmed S, Wu W, Gong JP. 2013. Characterization of internal fracture process of double network hydrogels under uniaxial elongation. *Soft Matter* 9:1955–66
69. Zhou Y, Hu J, Zhao P, Zhang W, Suo Z, Lu T. 2021. Flaw-sensitivity of a tough hydrogel under monotonic and cyclic loads. *J. Mech. Phys. Solids* 153:104483
70. Zhang W, Hu J, Yang H, Suo Z, Lu T. 2021. Fatigue-resistant adhesion II: swell tolerance. *Extreme Mech. Lett.* 43:101182
71. Sanoja GE, Morelle XP, Comtet J, Yeh CJ, Ciccotti M, Creton C. 2021. Why is mechanical fatigue different from toughness in elastomers? The role of damage by polymer chain scission. *Sci. Adv.* 7:eabg9410
72. Kim J, Steck J. 2022. Mechanofluorescence reveals fatigue in double-network elastomers. *Matter* 5:2545–47

73. Wang M-J. 1998. Effect of polymer-filler and filler-filler interactions on dynamic properties of filled vulcanizates. *Rubber Chem. Technol.* 71:520–89
74. Heinrich G, Klüppel M. 2002. Recent advances in the theory of filler networking in elastomers. In *Filled Elastomers Drug Delivery Systems*, pp. 1–44. Berlin: Springer
75. Chen Z, Zhang G, Luo Y, Suo Z. 2024. Rubber-glass nanocomposites fabricated using mixed emulsions. *PNAS* 121:e2322684121
76. Jang BZ, Uhlmann DR, Sande JBV. 1984. Ductile-brittle transition in polymers. *J. Appl. Polym. Sci.* 29:3409–20
77. Legrand DG. 1969. Crazing, yielding, and fracture of polymers. I. Ductile brittle transition in polycarbonate. *J. Appl. Polym. Sci.* 13:2129–47
78. Cheng WM, Miller GA, Manson JA, Hertzberg RW, Sperling LH. 1990. Mechanical behaviour of poly(methyl methacrylate). Part 1: tensile strength and fracture toughness. *J. Mater. Sci.* 25:1917–23
79. Cox HL. 1952. The elasticity and strength of paper and other fibrous materials. *Br. J. Appl. Phys.* 3:72–79
80. Lavoie SR, Hassan S, Kim J, Yin T, Suo Z. 2021. Toughness of a composite in which sliding between fibers and matrix is rate-sensitive. *Extreme Mech. Lett.* 46:101317
81. Taylor HM. 1959. Tensile and tearing strength of cotton cloths. *J. Text. Inst. Trans.* 50:T161–88
82. Hamkins CP, Backer S. 1980. On the mechanisms of tearing in woven fabrics. *Text. Res. J.* 50:323–27
83. Realff ML, Boyce MC, Backer S. 1997. A micromechanical model of the tensile behavior of woven fabric. *Text. Res. J.* 67:445–59
84. Liu F, Suo Z, Tang J. 2022. How does a glass fabric tear under cyclic force? *J. Mech. Phys. Solids* 158:104659
85. Bree J. 1989. Plastic deformation of a closed tube due to interaction of pressure stresses and cyclic thermal stresses. *Int. J. Mech. Sci.* 31:865–92
86. Gupta RK, ed. 2023. *Specialty Polymers: Fundamentals, Properties, Applications and Advances*. Boca Raton, FL: CRC Press. 1st ed.
87. Malito LG, Arevalo S, Kozak A, Spiegelberg S, Bellare A, Pruitt L. 2018. Material properties of ultra-high molecular weight polyethylene: comparison of tension, compression, nanomechanics and microstructure across clinical formulations. *J. Mech. Behav. Biomed. Mater.* 83:9–19
88. Vasile C, Pascu M. 2005. *Practical Guide to Polyethylene*. Shrewsbury, UK: RAPRA Tech.
89. Yeh JT, Runt J. 1991. Fatigue crack propagation in high-density polyethylene. *J. Polym. Sci. B* 29:371–88
90. Cerpentier RRJ, Boerakker MJ, Tervoort TA, Van Drongelen M, Govaert LE. 2022. Influence of electron-beam irradiation on plasticity-controlled and crack-growth-controlled failure in high-density polyethylene. *J. Polym. Sci.* 60:701–14
91. Persson BNJ, Albohr O, Heinrich G, Ueba H. 2005. Crack propagation in rubber-like materials. *J. Phys. Condens. Matter* 17:R1071–142
92. Cadwell SM, Merrill RA, Sloman CM, Yost FL. 1940. Dynamic fatigue life of rubber. *Ind. Eng. Chem.* 13:304–15
93. Saintier N, Cailletaud G, Piques R. 2011. Cyclic loadings and crystallization of natural rubber: an explanation of fatigue crack propagation reinforcement under a positive loading ratio. *Mater. Sci. Eng. A* 528:1078–86
94. Liu C, Morimoto N, Jiang L, Kawahara S, Noritomi T, et al. 2021. Tough hydrogels with rapid self-reinforcement. *Science* 372:1078–81
95. Hartquist CM, Lin S, Zhang JH, Wang S, Rubinstein M, Zhao X. 2023. An elastomer with ultrahigh strain-induced crystallization. *Sci. Adv.* 9:eadj0411
96. Scetta G, Ju J, Selles N, Heuillet P, Ciccotti M, Creton C. 2021. Strain induced strengthening of soft thermoplastic polyurethanes under cyclic deformation. *J. Polym. Sci.* 59:685–96
97. Peppas NA, Hilt JZ, Khademhosseini A, Langer R. 2006. Hydrogels in biology and medicine: from molecular principles to bionanotechnology. *Adv. Mater.* 18:1345–60
98. Slaughter BV, Khurshid SS, Fisher OZ, Khademhosseini A, Peppas NA. 2009. Hydrogels in regenerative medicine. *Adv. Mater.* 21:3307–29
99. Peppas NA, Stauffer SR. 1991. Reinforced uncrosslinked poly (vinyl alcohol) gels produced by cyclic freezing-thawing processes: a short review. *J. Control. Release* 16:305–10

100. Hassan CM, Peppas NA. 2000. Structure and morphology of freeze/thawed PVA hydrogels. *Macromolecules* 33:2472–79
101. Lin S, Liu X, Liu J, Yuk H, Loh H-C, et al. 2019. Anti-fatigue-fracture hydrogels. *Sci. Adv.* 22:eaau8528
102. Bai R, Yang J, Morelle XP, Suo Z. 2019. Flaw-insensitive hydrogels under static and cyclic loads. *Macromol. Rapid Commun.* 40:1800883
103. Lin S, Liu J, Liu X, Zhao X. 2019. Muscle-like fatigue-resistant hydrogels by mechanical training. *PNAS* 116:10244–49
104. Hua M, Wu S, Ma Y, Zhao Y, Chen Z, et al. 2021. Strong tough hydrogels via the synergy of freeze-casting and salting out. *Nature* 590:594–99
105. Roland CM. 2013. Immiscible rubber blends. In *Advances in Elastomers I*, ed. PM Visakh, S Thomas, AK Chandra, AP Mathew, pp. 167–81. Berlin: Springer
106. Lu PJ, Zaccarelli E, Ciulla F, Schofield AB, Sciortino F, Weitz DA. 2008. Gelation of particles with short-range attraction. *Nature* 453:499–503
107. Leibler L. 1980. Theory of microphase separation in block copolymers. *Macromolecules* 13:1602–17
108. Fernández-Rico C, Sai T, Sicher A, Style RW, Dufresne ER. 2022. Putting the squeeze on phase separation. *JACS Au* 2:66–73
109. Wienk IM, Boom RM, Beerlage MAM, Bulte AMW, Smolders CA, Strathmann H. 1996. Recent advances in the formation of phase inversion membranes made from amorphous or semi-crystalline polymers. *J. Membr. Sci.* 113:361–71
110. Zaccarelli E. 2007. Colloidal gels: equilibrium and non-equilibrium routes. *J. Phys. Condens. Matter* 19:323101
111. Bates FS, Fredrickson GH. 1999. Block copolymers—designer soft materials. *Phys. Today* 52:32–38
112. Kim H-C, Park S-M, Hinsberg WD. 2010. Block copolymer based nanostructures: materials, processes, and applications to electronics. *Chem. Rev.* 110:146–77
113. Zhang G, Kim J, Hassan S, Suo Z. 2022. Self-assembled nanocomposites of high water content and load-bearing capacity. *PNAS* 119:e2203962119
114. Kusters GLA, Zhang G, Chen Z, Suo Z. 2023. Amphiphilic monomers bridge hydrophobic polymers and water. *Soft Matter* 19:9489–95
115. Kramer EJ. 1983. Microscopic and molecular fundamentals of crazing. In *Crazing in Polymers*, ed. HH Kausch, pp. 1–56. Berlin: Springer
116. Ivan'kova EM, Krumova M, Michler GH, Koets PP. 2004. Morphology and toughness of coextruded PS/PMMA multilayers. *Colloid Polym. Sci.* 282:203–8
117. Adhikari R, Michler GH. 2004. Influence of molecular architecture on morphology and micromechanical behavior of styrene/butadiene block copolymer systems. *Prog. Polym. Sci.* 29:949–86
118. Velez NR, Allen FI, Jones MA, Govindjee S, Meyers GF, Minor AM. 2020. Extreme ductility in freestanding polystyrene thin films. *Macromolecules* 53:8650–62
119. Ahn CH, Zhang G, Suo Z. 2024. Ductility of a nanocomposite of glassy and rubbery polymers. *J. Mech. Phys. Solids* 191:105760
120. Mars WV, Ellul MD. 2017. Fatigue characterization of a thermoplastic elastomer. *Rubber Chem. Technol.* 90:367–80
121. Li X, Cui K, Sun TL, Meng L, Yu C, et al. 2020. Mesoscale bicontinuous networks in self-healing hydrogels delay fatigue fracture. *PNAS* 117:7606–12
122. Li X, Cui K, Kurokawa T, Ye YN, Sun TL, et al. 2021. Effect of mesoscale phase contrast on fatigue-delaying behavior of self-healing hydrogels. *Sci. Adv.* 7:eabe8210
123. Zheng Y, Kiyama R, Matsuda T, Cui K, Li X, et al. 2021. Nanophase separation in immiscible double network elastomers induces synergetic strengthening, toughening, and fatigue- resistance. *Chem. Mater.* 39:3321–34
124. Zhang G, Steck J, Kim J, Ahn CH, Suo Z. 2023. Hydrogels of arrested phase separation simultaneously achieve high strength and low hysteresis. *Sci. Adv.* 9:eadh7742
125. Kim M, Zhang G, Jang S, Lee S, Suo Z, Kim SM. 2024. Fatigue-resistant polymer electrolyte membranes for fuel cells. *Adv. Mater.* 36:2308288
126. Mallick PK. 2007. *Fiber-Reinforced Composites: Materials, Manufacturing, and Design*. Boca Raton, FL: CRC Press. 3rd ed.

127. Goettler LA, Shen KS. 1983. Short fiber reinforced elastomers. *Rubber Chem. Technol.* 56:619–38
128. Sathishkumar T, Satheeshkumar S, Naveen J. 2014. Glass fiber-reinforced polymer composites—a review. *J. Reinf. Plast. Compos.* 33:1258–75
129. US Congr. Off. Technol. Assess. 1988. *Advanced Materials by Design*. Washington, DC: US Gov. Print. Off.
130. Wang R-M, Zheng S-R, Zheng YG. 2011. *Polymer Matrix Composites and Technology*. Philadelphia, PA: Woodhead Publ.
131. Cui W, Huang Y, Chen L, Zheng Y, Saruwatari Y, et al. 2021. Tiny yet tough: maximizing the toughness of fiber-reinforced soft composites in the absence of a fiber-fracture mechanism. *Matter* 4:3646–61
132. Cui W, King DR, Huang Y, Chen L, Sun TL, et al. 2020. Fiber-reinforced viscoelastomers show extraordinary crack resistance that exceeds metals. *Adv. Mater.* 32:1907180
133. Huang Y, King DR, Cui W, Sun TL, Guo H, et al. 2019. Superior fracture resistance of fiber reinforced polyampholyte hydrogels achieved by extraordinarily large energy-dissipative process zones. *J. Mater. Chem. A* 7:13431–40
134. Huang Y, King DR, Sun TL, Nonoyama T, Kurokawa T, et al. 2017. Energy-dissipative matrices enable synergistic toughening in fiber reinforced soft composites. *Adv. Funct. Mater.* 27:1605350
135. Hui C-Y, Liu Z, Phoenix SL, King DR, Cui W, et al. 2020. Mechanical behavior of unidirectional fiber reinforced soft composites. *Extreme Mech. Lett.* 35:100642
136. Hui C-Y, Liu Z, Phoenix SL. 2019. Size effect on elastic stress concentrations in unidirectional fiber reinforced soft composites. *Extreme Mech. Lett.* 33:100573
137. King DR, Sun TL, Huang Y, Kurokawa T, Nonoyama T, et al. 2015. Extremely tough composites from fabric reinforced polyampholyte hydrogels. *Mater. Horiz.* 2:584–91
138. Gamstedt EK, Östlund S. 2001. Fatigue propagation of fibre-bridged cracks in unidirectional polymer-matrix composites. *Appl. Compos. Mater.* 8:385–410
139. Monticeli FM, Fuga FR, Donadon MV. 2023. A systematic review on translaminar fracture damage propagation in fiber-reinforced polymer composites. *Thin-Walled Struct.* 187:110742
140. Brunner AJ, Murphy N, Pinter G. 2009. Development of a standardized procedure for the characterization of interlaminar delamination propagation in advanced composites under fatigue mode I loading conditions. *Eng. Fract. Mech.* 76:2678–89
141. Gao X, Umair M, Nawab Y, Latif Z, Ahmad S, et al. 2022. Mode I fatigue of fibre reinforced polymeric composites: a review. *Polymers* 14:4558
142. Yao L, Alderliesten RC, Jones R, Kinloch AJ. 2018. Delamination fatigue growth in polymer-matrix fibre composites: a methodology for determining the design and lifing allowables. *Compos. Struct.* 196:8–20
143. Pingkarawat K, Mouritz AP. 2014. Improving the mode I delamination fatigue resistance of composites using z-pins. *Compos. Sci. Technol.* 92:70–76
144. Lin S, Cao C, Wang Q, Gonzalez M, Dolbow JE, Zhao X. 2014. Design of stiff, tough and stretchy hydrogel composites via nanoscale hybrid crosslinking and macroscale fiber reinforcement. *Soft Matter* 10:7519–27
145. Wang Z, Xiang C, Yao X, Le Floch P, Mendez J, Suo Z. 2019. Stretchable materials of high toughness and low hysteresis. *PNAS* 116:5967–72
146. Zhang G, Yin T, Nian G, Suo Z. 2021. Fatigue-resistant polyurethane elastomer composites. *Extreme Mech. Lett.* 48:101434
147. Bao G, Suo Z. 1992. Remarks on crack-bridging concepts. *Appl. Mech. Rev.* 45:355–66
148. Li C, Yang H, Suo Z, Tang J. 2020. Fatigue-resistant elastomers. *J. Mech. Phys. Solids* 134:103751
149. O'Masta MR, Dong L, St-Pierre L, Wadley HNG, Deshpande VS. 2017. The fracture toughness of octet-truss lattices. *J. Mech. Phys. Solids* 98:271–89
150. Shaikeea AJD, Cui H, O'Masta M, Zheng XR, Deshpande VS. 2022. The toughness of mechanical metamaterials. *Nat. Mater.* 21:297–304
151. Zeng L, Liu F, Yu Q, Jin C, Yang J, et al. 2023. Flaw-insensitive fatigue resistance of chemically fixed collagenous soft tissues. *Sci. Adv.* 9:eade7375
152. Zhou Y, Lin S, Zhang X, Wu H, Blanchet J, et al. 2024. Is a high-throughput experimental dataset large enough to accurately estimate a statistic? *J. Mech. Phys. Solids* 183:105521

153. Wu H, Zhang X, Zhou Y, Blanchet J, Suo Z, Lu T. 2023. Detection and reduction of systematic bias in high-throughput rupture experiments. *J. Mech. Phys. Solids* 174:105249
154. Zhou Y, Zhang X, Yang M, Pan Y, Du Z, et al. 2022. High-throughput experiments for rare-event rupture of materials. *Matter* 5:654–65
155. Suresh S. 1998. *Fatigue of Materials*. Cambridge, UK: Cambridge Univ. Press. 2nd ed.
156. Suresh S, Ritchie RO. 1984. Propagation of short fatigue cracks. *Int. Met. Rev.* 29:445–75
157. Chen C, Wang Z, Suo Z. 2017. Flaw sensitivity of highly stretchable materials. *Extreme Mech. Lett.* 10:50–57
158. Tanrattanakul V, Sungthong N, Raksa P. 2008. Rubber toughening of nylon 6 with epoxidized natural rubber. *Polym. Test.* 27:794–800
159. Mu Q. 2022. Experimental data for creep and dynamic mechanical properties of polycarbonate and polycarbonate/acrylonitrile-butadiene-styrene. *Data Brief* 42:108264
160. Piggott M. 2002. *Load Bearing Fibre Composites*. New York: Kluwer
161. Sinclair A, Zhou X, Tangpong S, Bajwa DS, Quadir M, Jiang L. 2019. High-performance styrene-butadiene rubber nanocomposites reinforced by surface-modified cellulose nanofibers. *ACS Omega* 4:13189–99
162. Lamri A, Shirinbayan M, Pereira M, Truffault L, Fitoussi J, et al. 2020. Effects of strain rate and temperature on the mechanical behavior of high-density polyethylene. *J. Appl. Polym. Sci.* 137:48778
163. Ragosta G, Musto P, Martuscelli E, Russo P, Zeloni L. 2001. Recycling of a plastic car component having a multilayer structure: morphological and mechanical analysis. *J. Mater. Sci.* 36:1231–41
164. Zhu Q, Li D. 2019. Interface reinforcement of pulp fiber based ABS composite with hydrogen bonding initiated interlinked structure via alkaline oxidation and tert-butyl grafting on cellulose. *Polymers* 11:2048